IOPscience iopscience.iop.org

Home Search Collections Journals About Contact us My IOPscience

# Magnetic correlations in single-crystalline $CeNi_2Ge_2$

This article has been downloaded from IOPscience. Please scroll down to see the full text article.

2000 J. Phys.: Condens. Matter 12 5423

(http://iopscience.iop.org/0953-8984/12/25/307)

View the table of contents for this issue, or go to the journal homepage for more

Download details:
IP Address: 171.66.16.221
The article was downloaded on 16/05/2010 at 05:15

Please note that terms and conditions apply.

J. Phys.: Condens. Matter **12** (2000) 5423–5435. Printed in the UK PII: S0953-8984(00)12465-8

# Magnetic correlations in single-crystalline $CeNi_2Ge_2$

B Fåk†, J Flouquet†, G Lapertot†, T Fukuhara‡ and H Kadowaki§

† Commissariat à l'Energie Atomique, Département de Recherche Fondamentale sur la Matière Condensée, SPSMS, 38054 Grenoble, France
‡ Department of Liberal Arts and Science, Toyama Prefectural University, Kosugi, Toyama 939-02, Japan
§ Department of Physics, Tokyo Metropolitan University, Hachioji-shi, Tokyo 102-0397, Japan

Received 8 March 2000

**Abstract.** The antiferromagnetic correlations in the non-Fermi-liquid compound $CeNi_2Ge_2$ have been measured on single crystals using inelastic neutron scattering. The spin fluctuations with a characteristic energy of 4 meV are centred at the incommensurate wave vector (0.23, 0.23, 0.5), which is similar to where magnetic order develops in the related compound $CeCu_2Ge_2$. The magnetic correlations are anisotropic, with a quasi-two-dimensional extension along the [110] direction, implying that the moments are mostly correlated in the [110] planes. With increasing temperature, the correlated signal decreases, and above $T^* \approx 30$ K the magnetic scattering appears to be wave-vector independent.

## 1. Introduction

Landau Fermi-liquid theory has been outstandingly successful in describing low-temperature properties of normal and strongly correlated metals. The chief features for temperatures $T$ much below the characteristic Fermi temperature, $T_F$, are a specific heat that is linear in $T$, a resistivity that is quadratic in $T$ and a temperature-independent susceptibility. Today, an increasing number of strongly correlated electron system are being discovered that show deviations from Fermi-liquid behaviour at low temperatures [1, 2]. Specifically, the specific heat of these systems is of the form $C/T \propto \ln(T_0/T)$ or $C/T \propto \gamma_0 - \alpha\sqrt{T}$, while the resistivity is proportional to $T^\epsilon$ with $\epsilon < 2$. This so-called non-Fermi-liquid (NFL) behaviour can have several origins.

In uranium (5f) compounds, NFL behaviour is in general observed in doped compounds and appears to be related to single-ion properties, such as the two-channel quadrupolar Kondo effect or a disorder-induced distribution of Kondo temperatures $T_K$. In cerium (4f) compounds, and possibly also in some 3d metals, NFL behaviour is often considered to arise from the proximity of a zero-temperature second-order phase transition between a state with long-range magnetic order and a paramagnetic state, a so-called quantum critical point (QCP) [3–5]. The importance of disorder for the occurrence of NFL behaviour in 4f systems has been pointed out in both experimental [6] and theoretical [7] work, and most NFL Ce compounds are in fact non-stoichiometric. However, some systems show NFL behaviour without doping under applied pressure, such as $CePd_2Si_2$ and the 3d-electron system MnSi, while $CeNi_2Ge_2$ appears to be an NFL at zero pressure without doping.

A quantum critical point can be obtained in Ce compounds by tuning the effective exchange interaction $J$ that determines the relative strength of the RKKY interaction, which favours

0953-8984/00/255423+13$30.00 © 2000 IOP Publishing Ltd 

magnetic order, with respect to the Kondo effect, which screens the 4f moments due to spin-fluctuation effects. The tuning of $J$ can be achieved by applying external pressure, which through a change in the lattice parameters modifies the hybridization between the 4f and the conduction electrons, or by substitution, which creates a chemical pressure, changes (sometimes) the number of conduction electrons and introduces disorder. The best known example of NFL behaviour near a quantum critical point in Ce compounds is perhaps $CeCu_{5.9}Au_{0.1}$, where the low-temperature specific heat is given by $C/T \propto \ln(T_0/T)$ and the resistivity is linear in temperature [8]. While one would in general expect a $T^{3/2}$ power law in the low-temperature resistivity for a three-dimensional antiferromagnetic system close to a QCP, the observation of quasi-two-dimensional antiferromagnetic fluctuations [9] would explain the linear behaviour [10]. In this work, we are interested in $CeNi_2Ge_2$, which is close to a QCP and shows NFL behaviour without being disordered.

$CeNi_2Ge_2$, which crystallizes in a body-centred tetragonal structure, was originally reported as a common paramagnetic heavy-fermion compound, with an enhanced linear term in the specific heat of $\gamma = C/T = 350$ mJ K$^{-2}$ mol$^{-1}$ at $T = 0.3$ K and a Kondo temperature of about 30 K [11]. The first single-crystal studies reported an anisotropic resistivity with a $T^2$ dependence at low temperatures [12, 13] and an anisotropic static magnetic susceptibility with a maximum anisotropy $\chi_c/\chi_a \approx 2$ at $T = 30$ K [12–14]. A metamagnetic transition was observed at an applied magnetic field of 42 T at $T = 1.3$ K [13]. More detailed studies of $CeNi_2Ge_2$ samples with low residual resistivity showed clear deviations from Fermi-liquid behaviour, with a low-temperature resistivity of the form $\rho = \rho_0 + T^\epsilon$, where $\epsilon = 1.35$–$1.5$ at zero or small magnetic fields (<1 T) [15–18]. However, a recent study showed a cross-over behaviour with $\epsilon$ going from 1.35 to 2 on lowering the temperature from 0.2 to 0.1 K [19]. The non-Fermi-liquid behaviour in the resistivity also disappears with magnetic field and with increasing temperature (above ~2 K). Resistivity measurements under hydrostatic pressure have also been reported [17, 20–23], with the appearance of superconductivity at high pressure [21] and possibly also at zero pressure for some samples [22, 23]. However, the measured resistivities are strongly sample dependent, and there is currently no consensus on the intrinsic behaviour of the resistivity. NFL behaviour is also seen in the specific heat, where $C/T \propto -\ln T$ below $T = 5$ K [16, 18] or $C/T \propto \gamma_0 - \alpha\sqrt{T}$ for $T \leqslant 2$ K [14, 16]. Under applied magnetic field, this strong enhancement of the low-temperature part of $C/T$ decreases, and for fields of the order of 4 T $C/T$ becomes nearly temperature independent below 1 K. The proximity of $CeNi_2Ge_2$ to a magnetic instability is demonstrated by chemical substitution. When Ni is substituted by Cu (20%) or Pd (10%), the system orders antiferromagnetically [24–26].

Inelastic neutron scattering measurements on polycrystalline $CeNi_2Ge_2$ [11] showed a broad quasielastic contribution with a characteristic energy (relaxation rate) $\Gamma$ of about 4 meV, which was nearly independent of temperature. In contrast to many other heavy-fermion compounds, the quasielectric width does not decrease monotonically with decreasing temperature but remains at a constant finite value below $T = 60$ K. No wave-vector dependence of the magnetic scattering was observed, but such a $Q$-dependence would need to be very strong to be observed in polycrystalline samples. The crystal field Hamiltonian for $Ce^{3+}$ ions in tetragonal point symmetry splits the $J = 5/2$ Hund's rule ground state into three doublets. However, no crystal-field excitations have been observed in neutron scattering measurements [11].

In this work, we have characterized the magnetic correlations in single-crystalline $CeNi_2Ge_2$ by neutron inelastic scattering for energies between 1 and 7 meV as a function of wave vector $\boldsymbol{Q}$ and temperature $T$. Details on the sample growth and characterization and on the neutron scattering measurements are given in section 2. The experimental results are presented in section 3. A comparison is made with the Cu and Pd doped compounds in section 4 and a discussion of the main results (section 5) concludes the paper.

## 2. Experiment

$CeNi_2Ge_2$ crystallizes in the body-centred tetragonal $ThCr_2Si_2$ structure with space group $I4/mmm$ and room-temperature lattice parameters of $a = 4.15$ Å and $c = 9.842$ Å. Several single crystals with approximate dimensions of 4 mm diameter and 25 mm length were grown along the $c$-axis using the Czochralski method. Four of those crystals with a total weight of 9.8 g were mounted together and aligned with the [110] and [001] axes in the horizontal scattering plane. The mosaicity of the assembly was less than 0.5 degrees. The low-temperature zero-field resistivity measured on a piece cut from one of the crystals is well described by $\rho = \rho_0 + T^{\epsilon}$ for $0.5 < T < 1.0$ K with $\epsilon = 1.4 \pm 0.1$ and a residual resistivity of $\rho_0 = 2.5$ (3.3) $\mu\Omega$ cm for a current along the $a$- ($c$-) axis.

Inelastic neutron scattering measurements were made on several triple-axis spectrometers at the Institut Laue–Langevin (IN12 and IN22) and at the Laboratoire Léon Brillouin (4F2). Vertically focusing pyrolytic graphite PG(002) monochromators and horizontally focused PG(002) analysers were used in all cases with open collimations. The spectrometers were operated in W configuration with PG or Be filters to suppress higher-order neutrons in the incident (scattered) beam for fixed incident (scattered) wave vectors, which were 1.5, 1.64, 1.97, or 2.662 $Å^{-1}$, as detailed in the results section. The measurements were made in Orange cryostats at temperatures between 1.5 K and 200 K.

## 3. Results

As mentioned, Knopp *et al* [11] found magnetic scattering centred at an energy of 4 meV in polycrystalline $CeNi_2Ge_2$. We have characterized this magnetic response in reciprocal space using our single crystals. The measurements were concentrated on the $[1\bar{1}0]$ zone, which contains the [110] and [001] reciprocal lattice vectors (figure 1). This zone contains the propagation vectors for the magnetically ordered Pd and Cu doped compounds (see section 4).

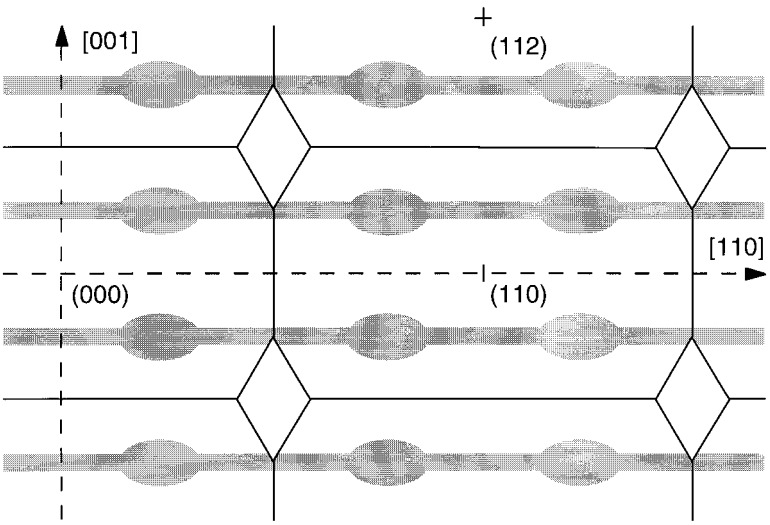


**Figure 1.** The reciprocal space spanned by [110] and [001] as studied in this work. The shaded areas correspond schematically to where the magnetic correlations are located.

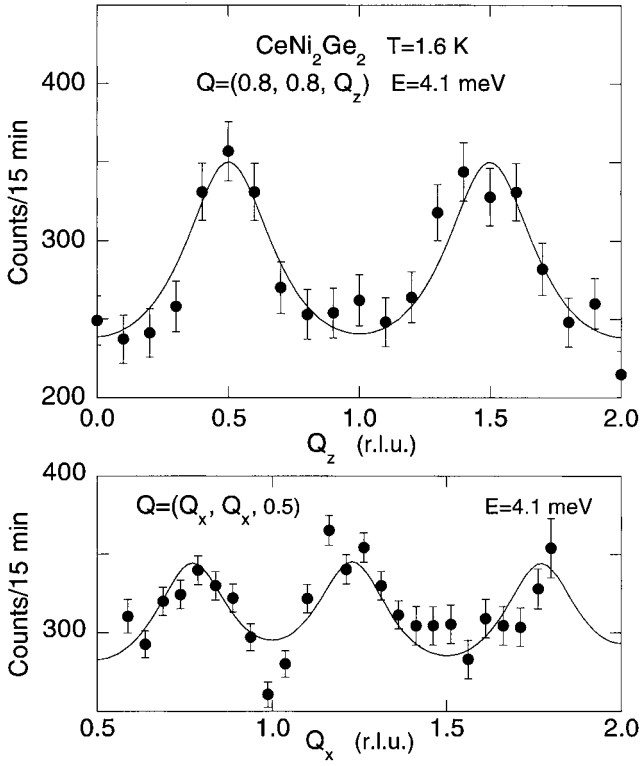


**Figure 2.** Scans along the [001] and [110] directions at 4.1 meV energy transfer at low temperatures show that the magnetic correlations are centred near $\boldsymbol{Q} = (0.77, 0.77, 0.5)$, i.e. the characteristic wave vector is $\boldsymbol{q}_0 = (0.23, 0.23, 0.5)$. The measurements were made on 4F2 with an incident energy of 14.7 meV.

Scans in the [110] and [001] directions (figure 2) show that the low-temperature magnetic correlations at an energy of 4 meV are broad in wave vector and centred at the reduced wave vector $\boldsymbol{q}_0 = (0.23, 0.23, 0.5)$. (We used the notation $\boldsymbol{Q} = \boldsymbol{\tau} + \boldsymbol{q}$, where $\boldsymbol{Q}$ is the total wave vector transferred from the neutron to the sample, $\boldsymbol{\tau}$ is a reciprocal lattice vector and $\boldsymbol{q}$ is the reduced wave vector which lies in the first Brillouin zone. The units are reduced lattice units, rlu.) The value of $\boldsymbol{q}_0$ is close to the propagation vector $\boldsymbol{k}$ for the magnetic structure in the $CeCu_2Ge_2$ compound, $\boldsymbol{k} = (0.28, 0.28, 0.54)$. The lines in figure 2 are fits of a sum of Lorentzians to the $\boldsymbol{Q}$-dependent intensity $I(\boldsymbol{Q})$,

$$I(\boldsymbol{Q}) = B + \sum \frac{I_0}{1 + [(\boldsymbol{Q} - \boldsymbol{\tau} \mp \boldsymbol{q}_0)/\kappa]^2} \tag{1}$$

where $B$ is the background, $I_0$ the magnitude of the magnetic scattering for the fixed energy transfer of the scan and $\kappa$ an estimate of the magnetic inverse correlation length. The sum is over the different reciprocal lattice vectors $\boldsymbol{\tau}$ (here (110)) and over $\pm\boldsymbol{q}_0$, the 'propagation vector' where the scattering is maximal. We obtain an inverse 'correlation length' of $\kappa_c = 0.22$ rlu or equivalently $\kappa_\perp = 0.14$ Å$^{-1}$ along the [001] direction, and $\kappa_\parallel = 0.26$ Å$^{-1}$ along the [110] direction. However, these values are somewhat misleading, since the scattering is considerably more extended along the [110] direction, as illustrated in figure 3(a), where peaks are seen for all scans in the [001] direction in the whole Brillouin zone, i.e. for all values of $Q_x$ at $\boldsymbol{Q} = (Q_x, Q_x, Q_z)$. This shows that the magnetic correlations have a strong anisotropy,

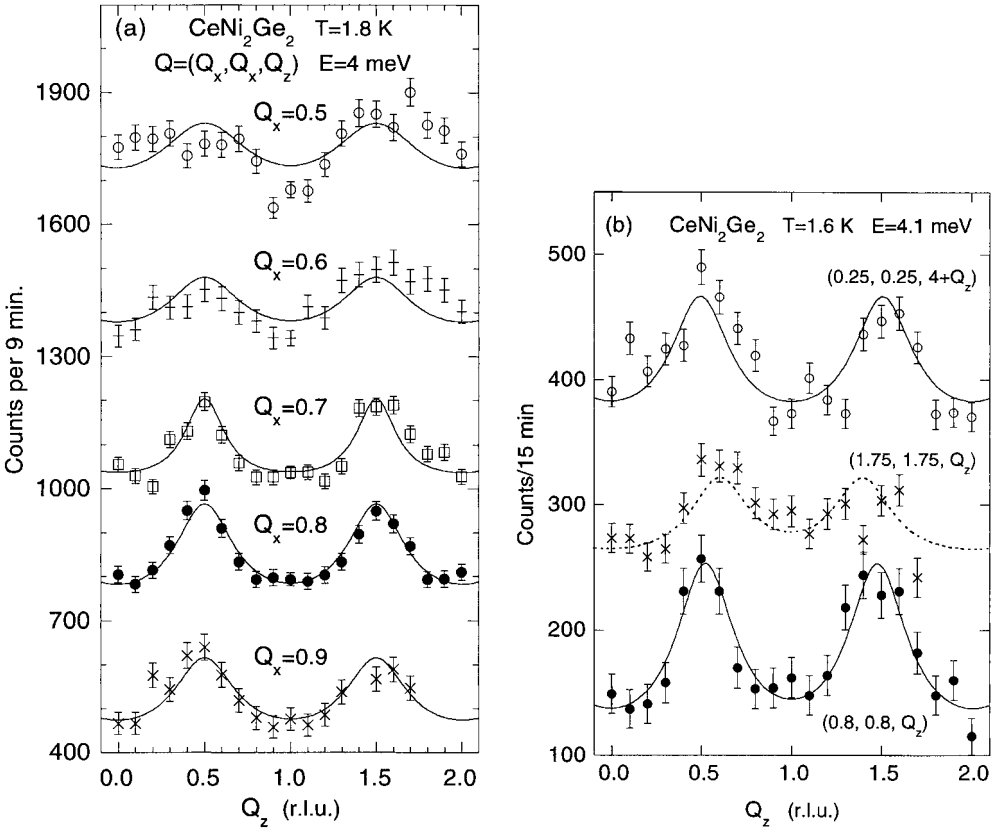


(a) (b)

**Figure 3.** (a) Scans along the [001] ($Q_z$) direction for different $Q_x$ values at $\boldsymbol{Q} = (Q_x, Q_x, Q_z)$ and 4 meV energy transfer at low temperatures. Magnetic correlations are observed for all $Q_x$-values, suggesting a quasi-two-dimensional character of the fluctuations. The different data sets have been shifted vertically by 300 counts between each set, except for the data set at $Q_x = 0.9$, which is not shifted. The measurements were made on IN22 with a final energy of 14.7 meV. (b) Scans along the [001] direction around the same reduced wave vector $\boldsymbol{q} = (1/4, 1/4, 1/2)$ at different positions $\boldsymbol{Q} = \boldsymbol{\tau} + \boldsymbol{q}$ in reciprocal space for 4 meV energy transfer at low temperatures. The top data set shows a scan centred at $\boldsymbol{Q} = (1/4, 1/4, 5)$, the middle at $\boldsymbol{Q} = (7/4, 7/4, 1)$, and the bottom at $\boldsymbol{Q} = (3/4, 3/4, 1)$. The upper and lower data sets have been shifted vertically by 100 counts with respect to the middle data set. The measurements were made on 4F2 with an incident energy of 14.7 meV.

with a tendency to quasi-two-dimensional behaviour with rods along the [110] direction. The magnetic moments are thus correlated in the [110] planes, with only small correlations between different [110] planes, as shown by the tendency to a better defined peak for $Q_x$-values of about 0.7–0.8 (figure 3(a)) or the small but clear peaking for scans in the [110] direction at $Q_x = 0.77$ (figure 2).

Since neutron scattering observes magnetic moments (or fluctuations) only perpendicular to the total wave vector $\boldsymbol{Q} = \boldsymbol{\tau} + \boldsymbol{q}$, the directions of these magnetic fluctuations can be found by measuring the same reduced wave vector $\boldsymbol{q}$ at different positions $\boldsymbol{Q}$ in reciprocal space. Figure 3(b) shows such scans. It can be seen that the magnetic intensity near $\boldsymbol{Q} = (1/4, 1/4, 5)$, where fluctuations in the basal plane of the tetragonal structure are observed ([110] plus [1$\bar{1}$0]), is nearly as strong as at the reference point (3/4, 3/4, 1), except for a reduction due to the

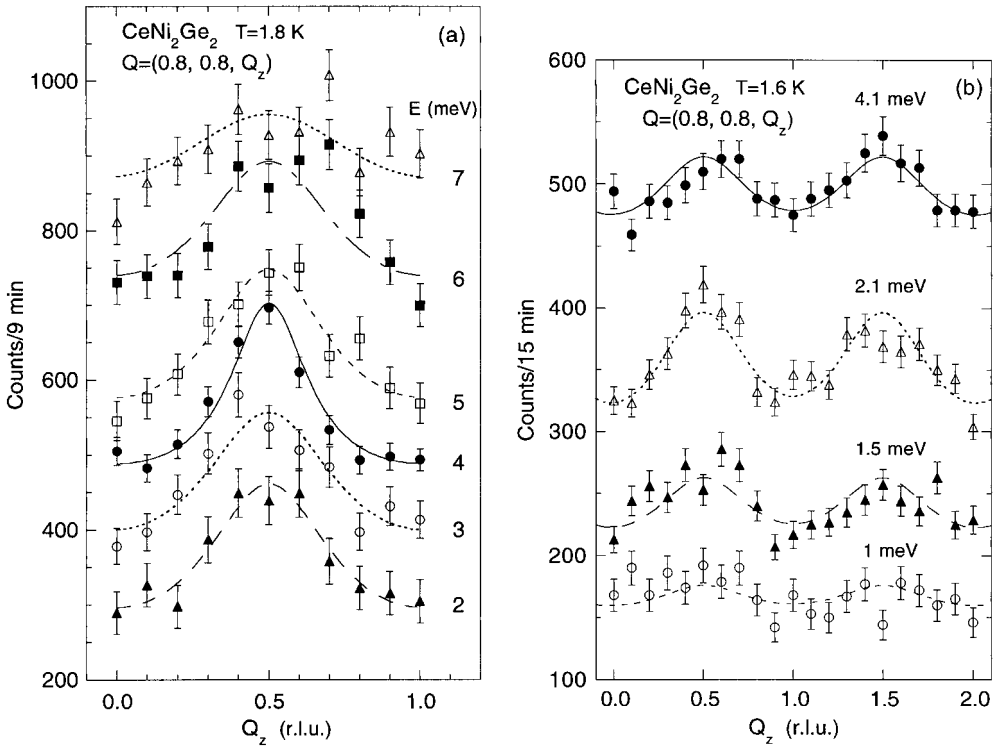


(a) (b)

**Figure 4.** Scans along the [001] direction through the (0.8, 0.8, 0.5) point at different energies and low temperatures. The lines are Lorentzian fits. (a) Measurements on IN22 with a final energy of 14.7 meV for energy transfers between 2 and 7 meV as shown on the right. The data sets have been shifted by 50 counts with respect to each other, except for the 4 meV set which is not shifted, and the 2 meV set which has been shifted down by 250 counts, due to the higher background from the tail of the elastic incoherent peak. (b) Measurements on 4F2 with a final energy of 8 meV for energy transfer between 1 and 4.1 meV. The data sets have been shifted by 100 counts with respect to each other, except for the data at 1 meV which are not shifted.

magnetic form factor. In contrast, the magnetic intensity is much weaker at (7/4, 7/4, 1), which has nearly the same $Q \equiv |\boldsymbol{Q}|$ value as (1/4, 1/4, 5) and hence the same magnetic form factor, but where fluctuations along the $[1\bar{1}0]$ and [001] directions are observed. The reduction in intensity by approximately a factor of two is what one expects if the magnetic moments are fluctuating in the basal plane only.

The energy range for the magnetic correlations has been investigated by scanning in the [001] direction at $\boldsymbol{Q} = (0.8, 0.8, 0.5)$ for different energies (figure 4). Magnetic correlations are clearly seen for energy transfers between 1.5 and 6 meV. For energies above 6 meV, the magnetic scattering becomes broad and it is difficult to distinguish it from the background and to separate it from scattering due to phonons. For energies below 2 meV, the amplitude of the magnetic signal decreases and the background increases due to the tail of the elastic incoherent scattering, and we have been unable to observe any magnetic correlations below 1 meV. However, we do not believe there is a gap in the magnetic excitation spectrum, only that the correlations in $\boldsymbol{Q}$ are smeared out at low energies or possibly have moved to another wave vector.

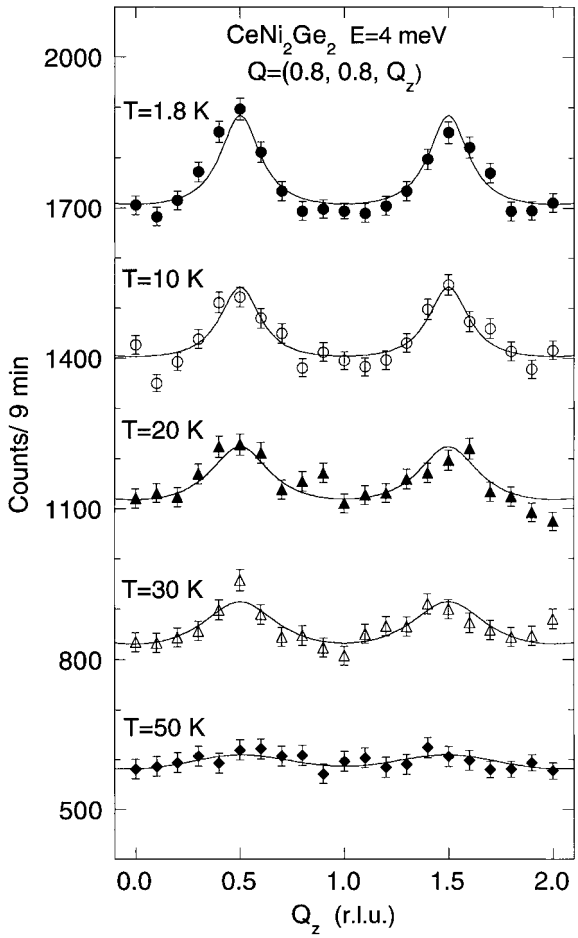


**Figure 5.** Temperature dependence of scans along the [001] direction through the $Q = (0.8, 0.8, 0.5)$ point at 4 meV energy transfer. The lines are Lorentzian fits. The measurements were made on IN22 with a final energy of 14.7 meV. The data sets have been shifted by 300 counts with respect to each other, except for the 50 K data which are not shifted.

The magnetic correlations disappear gradually with increasing temperature, as shown in figure 5 for scans along [001] at an energy of 4 meV. Similar results are obtained for scans at 2 meV (not shown). The $Q$-width of the correlations remains nearly constant, while the peak intensity decreases and the background increases. Above $T = 50$ K there are no longer any visible correlations, either in wave vector or in energy scans, although there is certainly broad uncorrelated magnetic scattering present. Knopp *et al* [11] observed indeed magnetic scattering in polycrystals up to 200 K, but could not study its $Q$-dependence.

It is difficult to extract the magnetic response from energy scans at a given wave vector due to the strong phonon contributions. At $\boldsymbol{Q} = (0.8, 0.8, 0.5)$, e.g., where the magnetic signal is maximal, there is one acoustic phonon at 7 meV and several phonon branches above 11 meV, as illustrated in figure 6(a). Since the magnetic scattering decreases, or at least becomes decorrelated with increasing temperature, one method is to subtract the high-temperature data

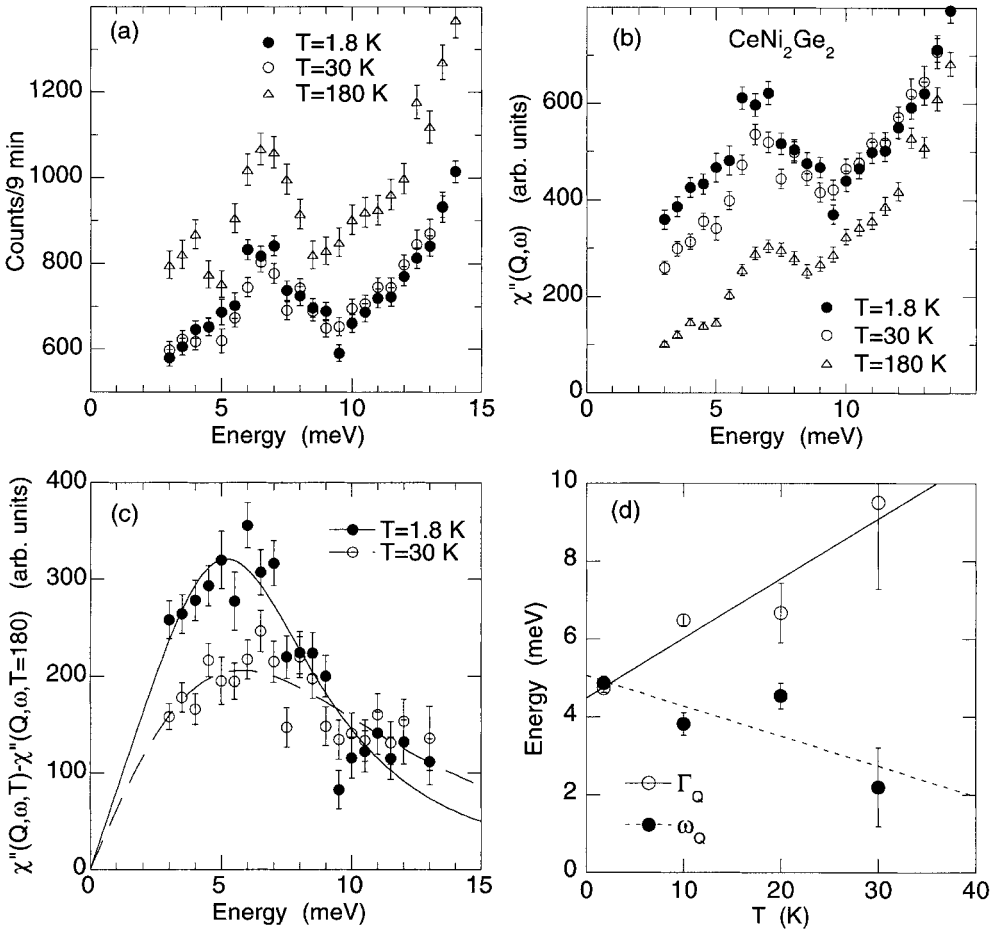


**Figure 6.** Energy response at $Q = (0.8, 0.8, 0.5)$ measured on IN22 with a final energy of 14.7 meV. (a) Raw data at different temperatures, showing phonon contributions at 7 meV and above 11 meV on top of a broad magnetic signal. (b) Dynamic susceptibility (magnetic plus phonon) after correcting the data in (a) for background and temperature factor. (c) Dynamic magnetic susceptibility after subtraction of the high-temperature ($T = 180$ K) phonon susceptibility shown in (b). The lines are fits to a damped harmonic oscillator. (d) Temperature dependence of the characteristic energy $\omega_q$ and damping $\Gamma_q$ of the magnetic susceptibility at $q = (0.2, 0.2, 0.5)$. The lines are linear fits.

from that at lower temperatures. For this, we assume that the observed intensity is given by

$$S(\boldsymbol{Q}, \omega) = [n(\omega) + 1][\chi''(\boldsymbol{Q}, \omega, T) + D(\boldsymbol{Q}, \omega, T)] + B \tag{2}$$

where $n(\omega)$ is the Bose factor, $\chi''$ the imaginary part of the dynamic magnetic susceptibility, $D$ the phonon scattering (also a dynamic susceptibility, strictly speaking) and $B$ a temperature independent background. After subtraction of the background, determined at negative energy transfers, and correction for the Bose factor, we obtain $\chi''(\boldsymbol{Q}, \omega, T) + D(\boldsymbol{Q}, \omega, T)$, shown in figure 6(b). As expected, the high-temperature data are dominated by the phonon contribution while the low-temperature data contain considerably more scattering at lower energies, presumed to be of magnetic origin. By subtracting the high-temperature data, which are assumed to have no *correlated* magnetic contribution, from the low-temperature data, we obtain

the dynamic magnetic susceptibility at low temperatures, shown in figure 6(c). The lines in the figure show that the data are well described by a damped harmonic oscillator,

$$\chi''(\boldsymbol{Q},\omega) = \frac{\chi'(\boldsymbol{Q})2\omega\Omega_q^2\Gamma_q}{(\omega^2-\Omega_q^2)^2+(2\omega\Gamma_q)^2} \tag{3}$$

where $\chi'(\boldsymbol{Q})$ is the $\boldsymbol{Q}$-dependent static susceptibility, $\Gamma_q$ the relaxation rate (or half-width) and $\omega_q = (\Omega_q^2+\Gamma_q^2)^{1/2}$ is the characteristic energy. Fits of this expression to energy scans at different wave vectors $\boldsymbol{Q} = (Q_x, Q_x, 0.5)$ show that $\Gamma_q$ and $\omega_q$ are independent of $Q_x$, while $\chi'(\boldsymbol{Q})$ decreases somewhat as $Q_x$ goes away from 0.77. The temperature dependence at $\Gamma_q$ and $\omega_q$ at $\boldsymbol{Q} = (0.8, 0.8, 0.5)$ is shown in figure 6(d). There is a slight increase in damping and a softening with increasing temperature.

## 4. Comparison with doped compounds

### *4.1. Magnetic order*

The magnetic structures and phase diagrams of Cu doped $CeNi_2Ge_2$ appear rather rich. In the pure $CeCu_2Ge_2$ compound, an incommensurate magnetic structure with a propagation vector of $\boldsymbol{k} = (0.28, 0.28, 0.54)$, a magnetic moment of 0.74 $\mu_B$ and a Néel temperature of 4.1 K was found in polycrystalline samples [27]. For low Ni concentrations in the doped compounds $Ce(Cu_{1-x}Ni_x)_2Ge_2$, two different magnetic phases were observed [24], with similar propagation vectors [28]. In a single crystal with $x = 0.5$, the propagation vector was found to be different, $\boldsymbol{k} = (0.5, 0.5, 0.8)$ [29], while for $x > 0.8$ no indications of magnetic order have been found [24, 29–31].

The broad correlations we have observed in $CeNi_2Ge_2$ correspond approximately to where magnetic order occurs in the pure $CeCu_2Ge_2$ compound, and not to that of the Ni doped samples. This is a sign of competition between different propagation vectors, which has already been observed in other Ce compounds. The best known example is $CeRu_2Si_2$, where magnetic correlations are observed at at least three different wave vectors, $\boldsymbol{k}_1 = (0.31, 0, 0)$, $\boldsymbol{k}_2 = (0.3, 0.3, 0)$ and $\boldsymbol{k}_3 = (0, 0, 0.35)$ [32, 33]. $CeRu_2Si_2$ becomes antiferromagnetically ordered for small doping: 8% La on the Ce site, 3% Rh on the Ru site or 5% Ge on the Si site, with the propagation vectors $\boldsymbol{k}_1$, $\boldsymbol{k}_3$ and $\boldsymbol{k}_1$, respectively [34–36].

The magnetic behaviour of the $Ce(Pd_{1-x}Ni_x)_2Ge_2$ series is considerably simpler. The pure compound $CePd_2Ge_2$ can be considered as a conventional antiferromagnet with no major spin-fluctuation effects, only a small enhancement of the linear term in the specific heat, and crystal field levels at 10 and 20 meV as deduced from macroscopic measurements [37]. To our knowledge, no inelastic neutron scattering measurements have been made on this system to study the crystal-field excitations, the quasielastic scattering above $T_N$ or the magnons in the ordered phase. Recent studies of the macroscopic properties of the polycrystalline $Ce(Pd_{1-x}Ni_x)_2Ge_2$ alloys [25, 26] show that for increasing Ni concentration the Néel temperature of 5.1 K for $x = 0$ decreases smoothly to 2 or 2.8 K for $x = 0.8$. The ground state is non-magnetic for $x \geqslant 0.9$, and shows NFL behaviour for $0.9 < x < 1$ in polycrystalline samples. In single crystals, the $x = 0.88$ compound is non-magnetic, but the resistivity cannot be described by $T^{\epsilon}$ using a fixed (temperature independent) $\epsilon$ [38]. The magnetic structure determinations by neutron diffraction on single crystals [39] and powder samples [40] show that $CePd_2Ge_2$ has a single-$\boldsymbol{k}$ collinear antiferromagnetic structure with a propagation vector $\boldsymbol{k} = (1/2, 1/2, 0)$ and the moments parallel to $\boldsymbol{k}$. This is the same structure as in $CePd_2Si_2$ [41, 42], and can be viewed as ferromagnetic (110) planes stacked antiferromagnetically with the moments normal to the planes. The ordered magnetic moment

at low temperatures is 0.86 $\mu_B$. The magnetic structure of $Ce(Pd_{1-x}Ni_x)_2Ge_2$ for $x = 0.65$ is similar with nearly the same propagation vector [39].

### *4.2. Magnetic inelastic scattering*

No crystal-field excitations were reported in the measurements on polycrystalline $CeNi_2Ge_2$ by Knopp *et al* [11]. In the Cu doped compound, on the other hand, an analysis of inelastic neutron scattering, specific heat and magnetic susceptibility measurements indicates that the crystal-field ground state of $Ce(Cu_{1-x}Ni_x)_2Ge_2$ for $x < 0.65$ is a doublet with two closely spaced doublets as excited states, separated from the ground state by approximately 16–19 meV, depending on the doping [27, 43]. The intensity of the crystal-field excitation decreases substantially with increasing Ni concentration [43].

Above the Néel temperature, the $Ce(Cu_{1-x}Ni_x)_2Ge_2$ compounds show quasielastic scattering with a weakly temperature-dependent magnetic relaxation rate of the order of 0.5–2.5 meV (depending on the doping and the temperature) [24, 27], corresponding approximately to the Kondo temperature. A non-Lorentzian line shape of the quasielastic scattering was observed in the pure $CeCu_2Ge_2$ compound below 30 K, pointing to short-range magnetic correlations [27]. For compounds containing Ni, no such deviations were observed [24].

## 5. Discussion

The main result of the present neutron scattering study of $CeNi_2Ge_2$ is the observation of magnetic correlations with a characteristic energy of 4 meV and a characteristic wave vector of $\boldsymbol{q}_0 = (0.23, 0.23, 0.5)$, which is similar to the ordering vector of $CeCu_2Ge_2$. The magnetic correlations have a quasi-two-dimensional character, where the moments in the [110] planes are correlated. From the wave-vector dependence of the magnetic correlations shown in figure 3(b), it appears as if the moments fluctuate predominantly in the basal plane, which is in apparent contradiction with static susceptibility measurements, where $\chi_c$ is two times larger than $\chi_a$. However, the quality of the data shown in that figure is quite limited. The correlations in wave vector $\boldsymbol{Q}$ disappear with increasing temperature, and it appears as if the magnetic scattering above $T = 30$ K is mainly isotropic and $Q$ independent, corresponding to local moment fluctuations.

Although we have been unsuccessful in establishing the detailed energy dependence of the dynamic susceptibility, our data are consistent with the finding by Knopp *et al* [11] on polycrystalline samples that the characteristic energy $\Gamma$ (or relaxation rate) is approximately 4 meV for temperatures up to at least 30 K. While $\Gamma$ in heavy-fermion Ce compounds in general increases with temperature, often according to $\Gamma(T) = \Gamma_0 + \alpha\sqrt{T}$, that of $CeNi_2Ge_2$ is nearly temperature independent with a small minimum at $T^* \approx 30$ K [11]. This minimum is at the same temperature $T^*$ as where the magnetic correlations disappear. While our data show that the magnetic correlations in wave vector disappear for temperature between 30 and 50 K, they suggest that $Q$-independent magnetic scattering exists above this temperature. This leads to a natural interpretation of $\Gamma(T)$ in $CeNi_2Ge_2$ as observed by Knopp *et al* as a change in the nature of the spin fluctuations at $T^*$. Above $T^*$, the spin fluctuations are localized and $Q$ independent with the standard form for the relaxation rate of $\Gamma(T) = \Gamma_0 + \alpha\sqrt{T}$, with $\Gamma_0$ being slightly smaller than 1 meV. Below $T^*$, quasi-2D correlations in $\boldsymbol{Q}$ develop with a temperature independent $\Gamma$. This behaviour is schematically shown in figure 7. This interpretation is further supported by the fact that there is a maximum in the static susceptibility (for a field parallel to the $c$-axis) at $T^*$, suggesting the onset of antiferromagnetic (or incommensurate) fluctuations at this temperature. We also note that there is a cross-over of the resistivity curves for currents along the $a$- and $c$-directions at $T^*$.

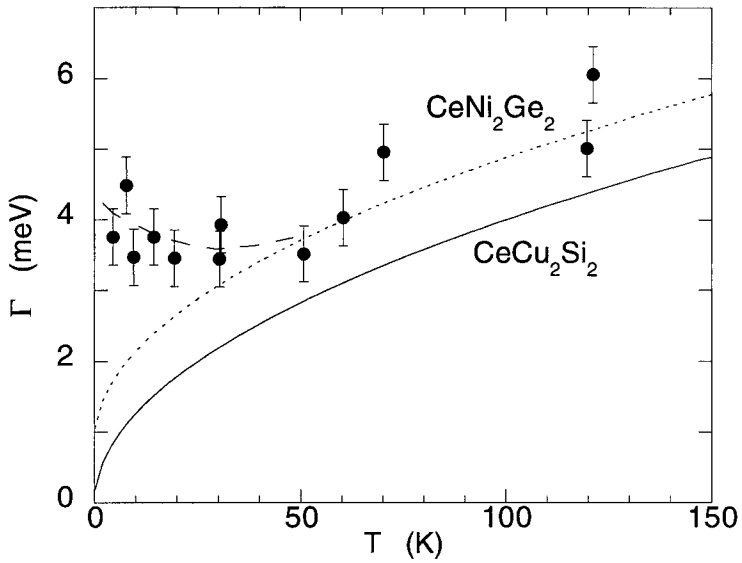


**Figure 7.** Quasielastic line width of the magnetic correlations in $CeNi_2Ge_2$ (after Knopp *et al* [11]). The dotted line shows the standard behaviour $\Gamma = 0.9 + 0.4\sqrt{T}$ modelled after $\Gamma = 0.4\sqrt{T}$ taken from $CeCu_2Si_2$ (solid line). Below $T^* \approx 30$ K, correlations in wave vector set in giving a temperature independent $\Gamma$.

The macroscopic properties of $CeNi_2Ge_2$ are quite similar to $CeRu_2Si_2$ [44]: both have a metamagnetic transition (42 versus 7.8 T), the same linear term in the specific heat ($\gamma = 350$ mJ K$^{-2}$ mol$^{-1}$), no well defined crystal field excitations, and an anisotropy that favours fluctuations along the $c$-axis, although the anisotropy is nearly Ising-like in $CeRu_2Si_2$ ($\chi_c/\chi_a = 20$ compared to 2 in $CeNi_2Ge_2$). Both are close to a magnetic instability, as shown by the doping studies discussed in section 4. Below $T = 0.8$ K, $CeRu_2Si_2$ shows Fermi-liquid behaviour with a constant $C/T$-term and a quadratic resistivity $\rho \propto T^2$. The overall behaviour of $CeRu_2Si_2$ is well described by a Moriya-type spin-fluctuation theory [45]. The corresponding low-energy magnetic correlations have been observed by inelastic neutron scattering experiments [32, 46]. $CeRu_2Si_2$ can thus be considered as being on the paramagnetic (Fermi-liquid) side of the quantum critical point in the Doniach phase diagram [47], although long-range magnetic order has been reported [48] with an extremely small moment. $CeNi_2Ge_2$ appears in this context to be closer to a quantum critical point, as a cross-over to a $T^2$ Fermi-liquid behaviour of the resistivity is observed only below $T = 0.1$ K, and the $\gamma$-term in the specific heat continues to increase with decreasing temperature down to at least 0.2 K. However, the spin fluctuations observed in this work are probably too high in energy (4 meV) to be related to the low-temperature properties of $CeNi_2Ge_2$.

The situation in $CeNi_2Ge_2$ bears some resemblance to $UPt_3$, another strongly correlated heavy-electron system ($\gamma \approx 400$ mJ K$^{-2}$ mol$^{-1}$) with incipient magnetic order ($\mu = 0.02\ \mu_B$ and $T_N = 5$ K) and unconventional superconductivity below $T_c \approx 0.5$ K. In $UPt_3$, antiferromagnetic correlations with a propagation vector of (0, 0, 1) and a characteristic energy of 5–8 meV set in at a temperature of about 17 K, where the static susceptibility has a maximum [49]. A second antiferromagnetic contribution occurs as a precursor of (and coexists with) the ordered moment, with a characteristic wave vector of (1/2, 0, 0) [50]. This scattering has a much lower energy scale, 0.5 meV, and the intensity is maximal at

$T = 5$ K. More recently, a third contribution was discovered at small $Q$-values, corresponding to ferromagnetic correlations with a dispersive quasielastic width, typically of the order of 1 meV [51]. One could speculate that in $CeNi_2Ge_2$, the magnetic correlations we have observed correspond to the first high-energy contribution in $UPt_3$, while other low-energy contributions corresponding to non-Fermi-liquid properties and/or precursor to magnetic order and superconductivity could be expected at some other wave vector.

The overall emerging picture of $CeNi_2Ge_2$ is thus a heavy-fermion system where low-energy antiferromagnetic fluctuations give rise to a finite relaxation time at low temperatures with non-Fermi-liquid behaviour of the specific heat and the resistivity. A small magnetic field, which probably acts to kill the low-energy spin fluctuations, suppresses this particular state, as does substitution of small amounts of Ni by Cu or isoelectronic Pd. This suggests that the NFL behaviour of $CeNi_2Ge_2$ is not due to impurity effects or a distribution of Kondo temperatures, but rather to the proximity of a magnetic–non-magnetic instability. Indeed, alloying with Cu or Pd on the Ni site induces magnetic order. In the Doniach phase diagram, $CeNi_2Ge_2$ is clearly on the (paramagnetic) Fermi-liquid side of the quantum critical point, but appears to be closer to the QCP than, e.g., La-doped $CeRu_2Si_2$. The antiferromagnetic correlations observed here by inelastic neutron scattering are probably not related to the NFL behaviour at low temperatures, since the energy scale (4 meV) is too high. These fluctuations appear however to be related to the maximum of the static susceptibility. One might expect the existence of low-energy spin fluctuations at some other competing wave vector, as observed in other strongly correlated electron systems. Such fluctuations have not yet been observed in $CeNi_2Ge_2$, either in our single-crystal studies or in measurements on polycrystals [11]. Future directions for studies of $CeNi_2Ge_2$ would be to search for low-energy magnetic correlations, determine the magnetic-field dependence of the spin fluctuations and try to approach the quantum critical point by alloying with, e.g., 5–10% Pd on the Ni site.

## Acknowledgments

We thank L P Regnault for precious help in the preparatory stages and A Georges, S Kambe, G Knebel, J M Mignot and S Raymond for discussions. Part of the neutron scattering measurements were carried out at the Laboratoire Léon Brillouin at CEA Saclay, Laboratoire Commun CEA–CNRS.

## References

[1] See, e.g. 1996 *Proc. Conf. on Non-Fermi Liquid Behavior in Metals, J. Phys.: Condens. Matter* **8**
[2] von Löhneysen H *et al* 1999 *J. Magn. Magn. Mater.* **200** 532
[3] Millis A J 1993 *Phys. Rev.* B **48** 7183
[4] Lonzarich G G 1994 *College on Quantum Phases (Trieste)*
[5] Moriya T and Takimoto T 1995 *J. Phys. Soc. Japan* **64** 960
[6] Graf T *et al* 1997 *Phys. Rev. Lett.* **78** 3769
[7] Castro Neto A H, Castilla G and Jones B A 1998 *Phys. Rev. Lett.* **81** 3531
[8] von Löhneysen H *et al* 1994 *Phys. Rev. Lett.* **72** 3262
von Löhneysen H 1996 *J. Phys.: Condens. Matter* **8** 9689
[9] Stockert O *et al* 1998 *Phys. Rev. Lett.* **80** 5627
Schröder A *et al* 1998 *Phys. Rev. Lett.* **80** 5623
[10] Rosch A, Schröder A, Stockert O and von Löhneysen H 1997 *Phys. Rev. Lett.* **79** 159
[11] Knopp G *et al* 1988 *J. Magn. Magn. Mater.* **74** 341
[12] Fukuhara T *et al* 1995 *J. Magn. Magn. Mater.* **140–144** 889. The labelling of the current directions in the resistivity curves of figure 1 is inverted.
[13] Fukuhara T *et al* 1996 *J. Phys. Soc. Japan* **65** 1559

[14] Aoki Y *et al* 1997 *J. Phys. Soc. Japan* **66** 2993
[15] Julian S R *et al* 1996 *J. Phys.: Condens. Matter* **8** 9675
[16] Steglich F *et al* 1996 *J. Phys.: Condens. Matter* **8** 9909
[17] Steglich F *et al* 1997 *Z. Phys.* B **103** 235
[18] Gegenwart P *et al* 1999 *Phys. Rev. Lett.* **82** 1293
[19] Julian S R *et al* 1998 *J. Magn. Magn. Mater.* **177–181** 265
[20] Fukuhara T *et al* 1997 *Physica* B **230–232** 198
[21] Grosche F M *et al* 1997 *Physica* B **239** 62
Lister S *et al* 1997 *Z. Phys.* B **103** 263
[22] Braithwaite D *et al* 2000 *J. Phys.: Condens. Matter* **12** 1339
[23] Grosche F M *et al* cond-mat/9812133
Gegenwart P *et al* 2000 *Physica* B **5** 281
[24] Loidl A *et al* 1992 *Ann. Phys., Lpz* **1** 78
[25] Fukuhara T *et al* 1998 *J. Phys. Soc. Japan* **67** 2084
[26] Knebel G *et al* 1999 *Phys. Rev.* B **59** 12 390
[27] Knopp G *et al* 1989 *Z. Phys.* B **77** 95
[28] Krimmel A 1993 private communication
[29] Sparn G *et al* 1997 *Physica* B **230–232** 317
[30] Knebel G *et al* 1997 *Physica* B **230–232** 593
[31] Buttgen N, Krug von Nidda H A and Loidl A 1997 *Physica* B **230–232** 590
[32] Regnault L P *et al* 1988 *Phys. Rev.* B **38** 4481
[33] Sato M *et al* 1999 *J. Phys. Chem. Solids* **60** 1203
[34] Quezel S *et al* 1988 *J. Magn. Magn. Mater.* **76/77** 403
[35] Miyako Y *et al* 1996 *Z. Phys.* B **101** 339
[36] Dakin S *et al* 1992 *J. Magn. Magn. Mater.* **108** 117
[37] Besnus M J *et al* 1992 *J. Magn. Magn. Mater.* **104–107** 1387
[38] Fukuhara T *et al* 1999 *Physica* B **259–261** 81
[39] Fåk B *et al Solid State Commun.* at press
[40] Feyerherm R *et al* 1998 *Physica* B **241–243** 643
[41] Steeman R A *et al* 1990 *J. Appl. Phys.* **67** 5203
[42] van Dijk N H *et al* 2000 *Phys. Rev.* B **61** 8922
[43] Krimmel A, Loidl A and Severing A 1997 *J. Phys.: Condens. Matter* **9** 873
[44] Flouquet J *et al* 1995 *Physica* B **215** 77 and references therein
[45] Kambe S 1996 *J. Phys. Soc. Japan* **65** 3294
[46] Raymond S *et al* 1997 *J. Low Temp. Phys.* **109** 205
[47] Doniach S 1977 *Physica* B **91** 213
[48] Amato A *et al* 1994 *Phys. Rev.* B **50** 619
[49] Aeppli G *et al* 1987 *Phys. Rev. Lett.* **58** 808
[50] Aeppli G *et al* 1988 *Phys. Rev. Lett.* **60** 615
[51] Bernhoeft N R and Lonzarich G G 1995 *J. Phys.: Condens. Matter* **7** 7325